Contents lists available at ScienceDirect

Chinese Chemical Letters

journal homepage: www.elsevier.com/locate/cclet

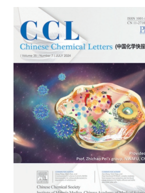

Luminescence-activated Pt(IV) prodrug for *in situ* triggerable cancer therapy

Huijie An[a,1], Chen Yang[a,1], Zhihui Jiang[a,1], Junjie Yuan[b], Zhongming Qiu[c], Longhao Chen[a], Xin Chen[a], Mutu Huang[a], Linlang Huang[a], Hongju Lin[a], Biao Cheng[a,*], Hongjiang Liu[d,*], Zhiqiang Yu[e,*]

[a] General Hospital of Southern Theatre Command, PLA, Guangzhou 510010, China
[b] The 925th Hospital of The Chinese People's Liberation Army, Guiyang 550025, China
[c] The 903rd Hospital of The People's Liberation Army, Hangzhou 310007, China
[d] The Second Hospital of Hebei Medical University, Shijiazhuang 050000, China
[e] The Tenth Affiliated Hospital of Southern Medical University (Dongguan people's hospital), Dongguan 523018, China

A R T I C L E I N F O

Article history:
Received 27 July 2023
Revised 19 September 2023
Accepted 20 September 2023
Available online 21 September 2023

Keywords:
Tumor microenvironment
Endogenous luminescence
Platinum(IV) prodrug
Activation strategy
Antitumor
Biosafety

A B S T R A C T

Anticancer platinum prodrugs that can be controllably activated are highly desired for personalized precision medicine and patient compliance in cancer therapy. However, the clinical application of platinum(IV) prodrugs (Pt(IV)) is restricted by tissue penetration of external irradiation. Here, we report a novel Pt(IV) activation strategy based on endogenous luminescence of tumor microenvironment responsiveness, which completely circumvents the limitation of external irradiation. The designed Pt(IV)–Lu, a mixture of *trans*, *trans*, *trans*-[Pt(N_3)$_2$(OH)$_2$(py)$_2$] and luminol (Lu), has controllable activation property: it remains inert in reductant environment and normal tissues, but under tumor microenvironment, Lu will be oxidized to produce blue luminescence, which rapidly reduce Pt(IV) to Pt(II) without the need of any external activator. Pt(IV)–Lu shows excellent responsive antitumor ability both *in vitro* and *in vivo*. Compared to cisplatin, the median lethal dose in BALB/c mice increased by an order of magnitude. Our results suggest that Pt(IV)–Lu exhibits highly controllable activation property, superior antitumor activity, and good biosafety, which may provide a novel strategy for the design of platinum prodrugs.

© 2024 Published by Elsevier B.V. on behalf of Chinese Chemical Society and Institute of Materia Medica, Chinese Academy of Medical Sciences.

As a DNA cross-linking molecule with excellent antitumor activity, platinum(II)-based drugs (Pt(II)) have become a mainstay in cancer chemotherapy [1,2]. Unfortunately, the low selectivity of Pt(II) towards tumor leads to non-negligible toxicity, such as nephrotoxicity, peripheral neurotoxicity, and ototoxicity, which causes undue harm to patients and hinders the full realization of its enormous potential. Recently, photoactivatable platinum(IV) prodrugs (Pt(IV)) design has received increasing attention [3]. The octahedral Pt(IV) is inert in the bloodstream, and can be selectively activated by light irradiation instead of reductants which are commonly found in cells, such as glutathione, thus minimizing unwanted activation [4,5]. In addition, the axial ligands of Pt(IV) can be modified to achieve desired biological properties such as targeting and hydrophilicity [6,7]. Ultraviolet light shows the strongest activation ability of conventional photoactivatable Pt(IV). However, the tissue penetration of ultraviolet light is poor, which highly restricts the application in deep tumors in clinic [8]. Efforts have been made to solve the problem. For example, introduced by pyridine group or fluorescent group with electron transfer ability, Pt(IV) can be activated by blue, or even red light, which has stronger penetrability [5,9–11]. In addition, upconversion nanoparticles are designed to activate Pt(IV) indirectly by converting near-infrared light to ultraviolet light [12,13]. Nevertheless, these strategies have not yet broken through the tissue penetration depth limit of exogenous light.

Unique pathological microenvironment of tumors, including elevated levels of reactive oxygen species (ROS) [14], enzymes [15], hypoxia [16], and low pH [17], has been utilized as endogenous activator to activate prodrugs. For example, the biosafety small molecule luminol (Lu) can produce blue luminescence in the tumor oxidative microenvironment, allowing early diagnosis of breast cancer and even its lung metastasis [18,19]. Meanwhile, this phenomenon provides a useful strategy for designing prodrugs with specific activation property in tumors [20–22]. Our previous research has confirmed that the blue luminescence emitted by Lu

* Corresponding authors.
E-mail addresses: chengbiaocheng@163.com (B. Cheng), willliu0414@163.com (H. Liu), zhiqiang.yu.1@asu.edu (Z. Yu).
[1] These authors contributed equally to this work.

https://doi.org/10.1016/j.cclet.2023.109134
1001-8417/© 2024 Published by Elsevier B.V. on behalf of Chinese Chemical Society and Institute of Materia Medica, Chinese Academy of Medical Sciences.

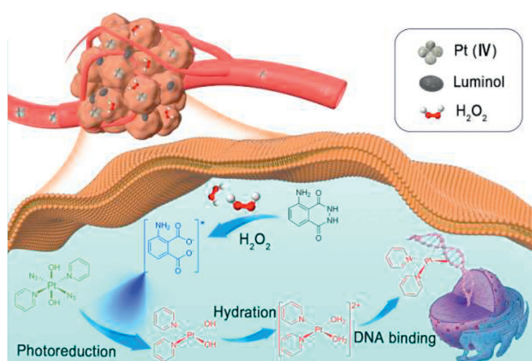

Scheme 1. Tumor treatment using Pt(IV) activated by responsive endogenous light in the tumor microenvironment.

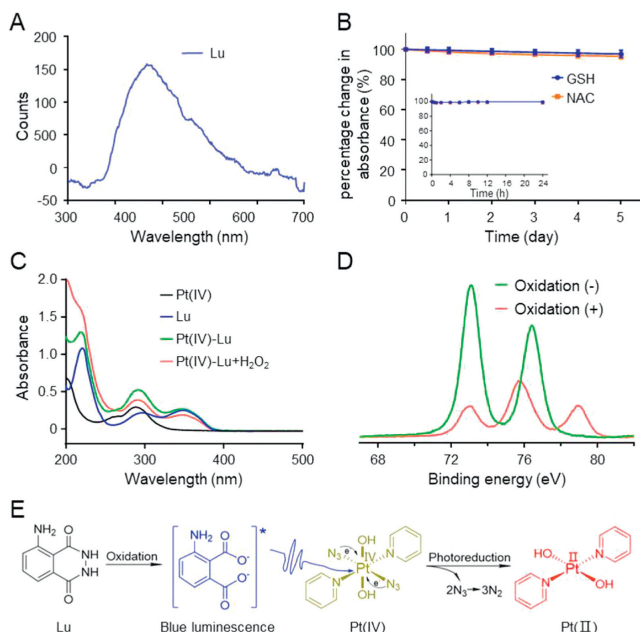

Fig. 1. Luminescence property of Lu and tability, luminescence activation behavior of Pt(IV). (A) Luminescent spectra of Lu. (B) Changes in the absorption of Pt(IV) at 289 nm after incubation in different reducing solutions for varied periods of time ($n = 3$). Data are presented as mean±standard deviation (SD). (C) UV–vis absorption spectra of Pt(IV), Lu, and Pt(IV)–Lu with or without 10 mmol/L H_2O_2. (D) XPS curves of Pt_{4f} in Pt(IV)–Lu before and after oxidation with 10 mmol/L H_2O_2. (E) Schematic illustration of luminescence activation mechanism of Pt(IV).

could be used as an endogenous light to activate the photosensitizer chlorin e6 and achieve photodynamic therapy in tumors [21,22]. This strategy can effectively solve the problem of tissue penetration of light sources. Above all, we hypothesized that the blue luminescence of Lu could be used as an endogenous light source to intelligently activate photoactivatable Pt(IV) and realize tumor chemotherapy without external light (Scheme 1).

In order to be efficiently activated by endogenous luminescence from Lu, *trans,trans,trans*-$[Pt(N_3)_2(OH)_2(py)_2]$ was selected as the Pt(IV) prodrug. In the presence of H_2O_2, Lu showed luminescence spectrum from 390 nm to 530 nm (Fig. 1A). This result theoretically suggests that Lu can be used as luminescence substrate to control the activation of *trans,trans,trans*-$[Pt(N_3)_2(OH)_2(py)_2]$, which can be photoactivated by lights over a wide range of wavelengths (from ultraviolet (UV) to visible (vis) light) [5,11]. The existence of planar pyridine ligands in Pt(IV) has a critical effect on the photoactivation pathways, matching and transferring the energy from luminescence to the Pt center to facilitate the reduction [5]. Meanwhile, the sterically hindered pyridines remain strongly bound to platinum even after photoactivation, which effectively reduces the ability of DNA to repair its own damage [5,11].

Then we tested this hypothesis by administering Pt(IV)–Lu, a mixture of *trans,trans,trans*-$[Pt(N_3)_2(OH)_2(py)_2]$ and Lu. The synthetic steps and structural characterization of *trans,trans,trans,trans,trans*-$[Pt(N_3)_2(OH)_2(py)_2]$ are provided in Figs. S1–S3 (Supporting information). The stability of Pt(IV) was examined first in the dark. Some types of Pt(IV) prodrugs can be reduced by intracellular reductants and easy to cause toxicity and side effects in the circulation, while Pt(IV) containing azide ligands (Pt–N_3) did not cause these problems. Hence, the absorption change of Pt–N_3 at 289 nm was monitored by UV–vis spectrophotometer to test the stability of Pt(IV). After incubation for 24 h in the presence of 5 mmol/L *N*-acetyl cysteine (NAC) or 5 mmol/L glutathione (GSH), 96% or 95% of Pt(IV) still remained, respectively. In addition, more than 90% of Pt(IV) still reminded when the incubation time was extended to 5 days in the dark (Fig. 1B and Fig. S4 in Supporting information), indicating that the prodrug is quite stable even in the presence of the reducing agent for a long time, which is advantageous for application *in vivo*.

The luminescence activation property of Pt(IV) was subsequently investigated. Pt(IV)–Lu showed characteristic absorption peak at 289 nm, which was the addition peak of Lu and Pt–N_3. However, the absorption peak was obviously decreased after oxidation with 10 mmol/L H_2O_2 (Fig. 1C). Additionally, the oxidation state change of Pt in the Pt(IV)–Lu before and after oxidation were obtained by X-ray photoelectron spectroscopy (XPS). The Pt_{4f} peaks in Pt(IV)–Lu exhibited the characteristic binding energies of 76.4 and 73.1 eV before oxidation, which were changed to 78.9, 75.6 and 73 eV after oxidation with 10 mmol/L H_2O_2 overnight (Fig. 1D). The successful activation of Pt(IV) was further confirmed by electrospray ionization mass spectrometry (ESI MS) analysis. The typical peak at *m/z* about 389.4 could be attributed to its molecular ion of $[Pt(II)+2H]^{2+}$, which was almost identical to the theoretical value (Fig. S5 in Supporting information). The above indicates that Pt(IV) in Pt(IV)–Lu can be luminescence-activated to Pt(II) after oxidation, along with the depletion of Lu and dissociation of the azide ligands.

Given the above observations, we tried to explain the possible mechanism of activation properties of Pt(IV). Since no spectral overlap was observed between the luminescence spectrum of Lu (max = 433 nm) and the absorption spectrum of Pt(IV) (max = 284 nm) (Fig. S6 in Supporting information), direct energy transfer between them is not likely to occur. As Lu is able to serves as a luminescence substrate that can be oxidized by H_2O_2 to yield a high-energy excited state of the aminophthalate ion, which may result in a direct electron transfer from the excited state of aminophthalate ion to the Pt(IV) center through photo-induced electron transfer (Fig. 1E).

Cell counting kit-8 (CCK8) assay was executed to detect the *in vitro* cellular proliferation inhibition and cytotoxicity in cancer cell (4T1, mouse breast cancer cell) and normal cell (human umbilical vein endothelial cell, HUVEC) under dark. Cisplatin and Pt(IV)–Lu + H_2O_2 exhibited significant cytotoxicity of similar degree on 4T1 cells, and their half-maximal inhibitory concentration (IC_{50}) were 7.58 and 19.56 μmol/L, respectively (Fig. 2A). In addition, Pt(IV) and Lu + H_2O_2 have little effect on proliferation of 4T1 cells. Compared with Figs. 2A and B, although Pt(IV)–Lu has a limited effect on 4T1 cells and HUVEC cells, it seems have a greater impact on 4T1 cells. These may take advantage of the fact that cancer cells can produce a considerable amount of oxidants even cultured *in vitro* without stimulation that can activate Pt(IV)–Lu to a certain extent [23]. The content of Pt-DNA adducts in Pt(IV)–Lu + H_2O_2 treated 4T1 cells was similar to that of cisplatin treated group, which is 4.16- or 2.16-fold higher than that in Pt(IV) treated and Pt(IV)–Lu treated ones (Fig. 2C).

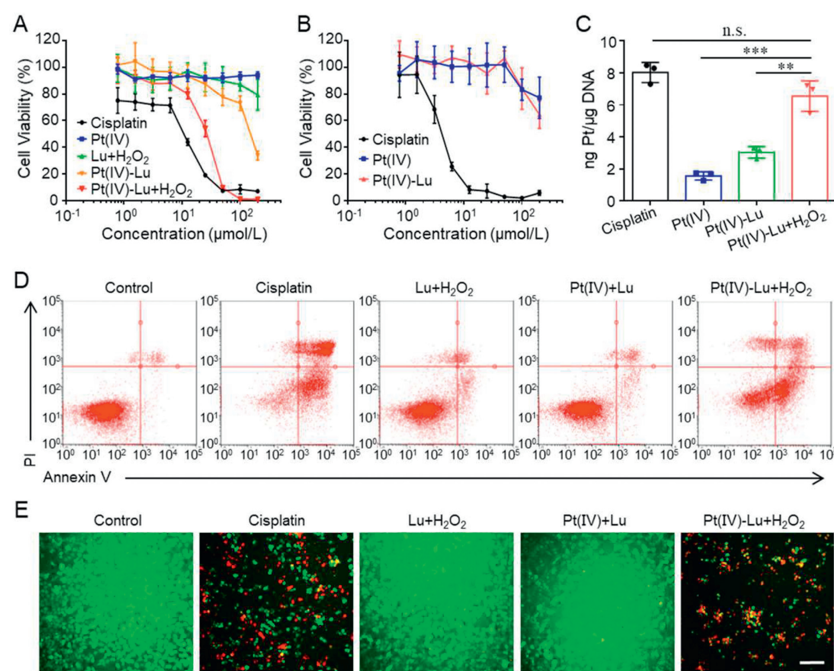

Fig. 2. Cytotoxicity of Pt(IV)–Lu. (A) 4T1 cells and (B) HUVEC cells viability after different treatments for 48 h ($n = 5$). (C) Accumulation of DNA-Pt adducts in 4T1 cells ($n = 3$). (D) Representative flow cytometric profiles of 4T1 cells with various treatments. (E) Detection of 4T1 cells damage by fluorescence microscopy using fluorescent probes (double-staining with calcein PI and calcein-AM). Dead cells: red fluorescence of PI, live cells: green fluorescence of calcein-AM, scale bar: 100 μm. Data are presented as mean±SD. $^{**}P < 0.01$, $^{***}P < 0.001$. n.s., no significance.

To further verify the responsive cytotoxicity caused by Pt(IV)–Lu, the cell apoptosis and necrosis analyses of 4T1 cells were conducted by staining with annexin V-fluorescein isothiocyanate (FITC) and propidium iodide (PI) (Fig. 2D and Fig. S7 in Supporting information). As expected, the ratio of apoptosis and necrosis was 60.1% when the cells were exposed to Pt(IV)–Lu + H_2O_2, which was 72.5% of that in group cisplatin. When 4T1 cells were treated with Pt(IV)–Lu without oxidant, the ratio of apoptosis and necrosis was 13.4%, which was not statistically different from that in control group.

Furthermore, 4T1 cells were stained with Calcein-AM and PI to visually detect the live and dead cells. As anticipated, compared with control, there was striking red fluorescence signals emitted from the cells treated with cisplatin or Pt(IV)–Lu + H_2O_2, while a slight red fluorescence was detected when treated with Pt(IV)–Lu or Lu + H_2O_2 (Fig. 2E and Fig. S8 in Supporting information).

The experimental results of the CCK8 assay, apoptosis assay and calcein-AM/PI taining assay were consistent, revealing that Pt(IV)–Lu supposedly exists in its intact Pt(IV) form in normal cells under dark, but can release biologically active Pt(II) under oxidation. Such a stable Pt(IV)–Lu holds promise for killing in target sites and minimizing the side effects through the specific activation of intelligent response.

In vivo antitumor efficacy was assessed in 4T1 bearing mice. All animal studies were performed in accordance with animal protocol procedures of Southern Medical University and approved by the Institutional Animal Care and Use Committee (IACUC). The mice were divided into five groups and treated with (1) phosphate buffer solution (PBS), (2) cisplatin (2.5 mg Pt/kg), (3) Lu (5 mg/kg), (4) Pt(IV) (2.5 mg Pt/kg), and (5) Pt(IV)–Lu (2.5 mg Pt/kg; 5 mg/kg Lu) every other day for a total of three times. As shown in Fig. 3A, tumor volume of the PBS group increased rapidly to ~1740 mm^3 on day 18, whereas administration of Lu and Pt(IV) showed weaker suppression of tumors (~1830 mm^3 and ~1361 mm^3, respectively). In comparison, the free cisplatin revealed significantly greater tumor growth inhibition (with an average volume of ~533 mm^3). Interestingly, compared with the free cisplatin, the Pt(IV)–Lu treated group revealed similar tumor growth inhibition (~720 mm^3). At the endpoint of treatment, all mice were euthanized and the collected tumors were photographed and weighed (Figs. 3B and C). The average tumor weights of mice treated with cisplatin or Pt(IV)–Lu were 0.56 ± 0.22 g and 0.75 ± 0.22 g, respectively, much lower than that of the other treated groups. The Pt-DNA adducts formed in tumor were detected by ICP-MS, and the results showed that Pt(IV)–Lu group had the similar Pt-DNA adduct formation (4.488 ng Pt/μg tumor DNA) compared with that of cisplatin treated groups (5.178 ng Pt/μg tumor DNA) (Fig. 3D), indicating the Pt(IV) could be reduced to active Pt(II) by blue luminescence of Lu under oxidation conditions. Moreover, the haematoxylin and eosin (H&E) staining and terminal deoxynucleotidyl transferase-mediated deoxyuridine triphosphate nick end labeling (TUNEL) staining of tumor sections from various groups showed compared with the control group, the tumor cells under cisplatin treatment or Pt(IV)–Lu treatment shrunk, appeared larger necrotic areas and apoptotic cancer cells (Fig. 3E).

Non-negligible toxicity of cisplatin cause undue harm to patients and hinder the full realization of its enormous potential. In here, the side effects of different treatments *in vivo* were verified. The acute toxicity experiments showed the median lethal dose (LD_{50}) of Pt(IV) was 50 mg Pt/kg, which was 10 times higher than that of cisplatin (5 mg Pt/kg) (Fig. 4A). Meanwhile, during *in vivo* anticancer experiment, all tested groups showed an increase in body weight, except for cisplatin, which had an average weight loss of 20.9% on day 6 (Fig. 4B). The biosafety was investigated by testing blood biochemistry parameters. Pt(IV)–Lu did not show obvious hepatotoxicity and nephrotoxicity, since normal levels of alanine aminotransferase (ALT), aspartate aminotransferase (AST), creatine (CREAT), and urea nitrogen (UREA) were observed. By contrast, the mice treated with cisplatin showed low level of CREAT and high level of UREA, indicated the severe renal toxicity induced by free cisplatin (Figs. 4C and D). In addition, at endpoint of treatment (day 18), H&E analysis revealed obvious glomerular injury in kidney after cisplatin administration, whereas there were no noticeable pathological changes of the major organs with other

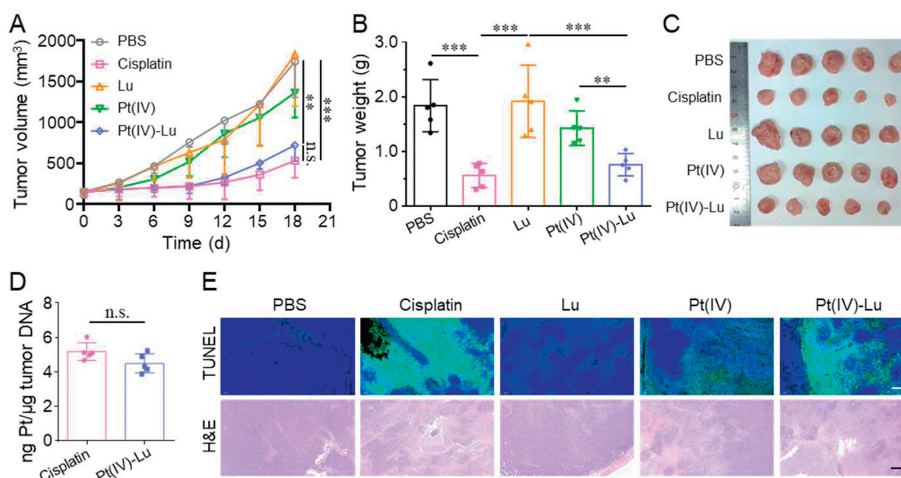

Fig. 3. Antitumor activity study of Pt(IV)–Lu in 4T1-tumor-bearing mice. (A) Changes in the tumor volume during treatment with PBS, cisplatin, Lu, Pt(IV), Pt(IV)–Lu (Pt-equiv. dose, 2.5 mg/kg) three time ($n = 5$). (B) The quantified tumor weight and (C) digital photo of excised tumors at 18 d after different treatments ($n = 5$). (D) Accumulation of DNA-Pt adducts in tumors on day 18 ($n = 5$). (E) TUNEL (scale bar: 200 μm) and H&E (scale bar: 400 μm) analysis of tumor sections isolated from mice on day 18. Data are presented as mean±SD. $^{**}P < 0.01$, $^{***}P < 0.001$.

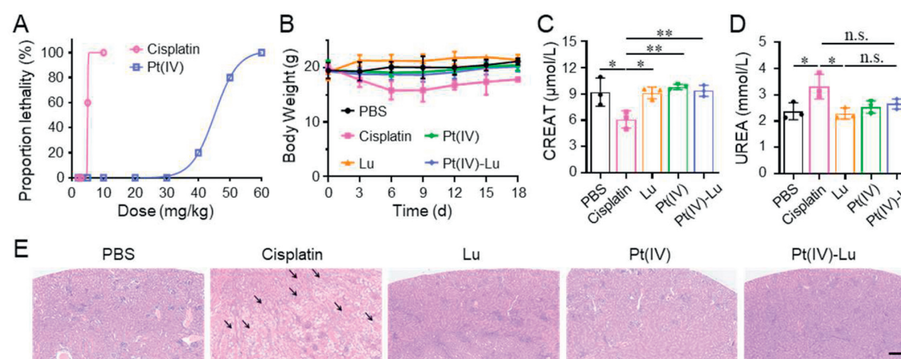

Fig. 4. Biosatety of Pt(IV)–Lu. (A) Probit model of 7-d survival after injection of different doses of cisplatin or Pt(IV). (B) Body weight change of mice during antitumor activity study ($n = 5$). (C) CREAT, (D) UREA and (E) H&E staining of kidneys of 4T1bearing mice treated with different formulations. The black arrows indicated renal tubular injury, scale bar: 200 μm. Data are presented as mean±SD. $^{*}P < 0.05$, $^{**}P < 0.01$.

treatment (Fig. 4E and Fig. S9 in Supporting information). All the above results demonstrated that Pt(IV)–Lu not only owned the similar antitumor efficiency as cisplatin, but also can greatly reduce systematic toxicity.

In summary, our study proposed a new strategy for activating the Pt(IV) prodrug for the first time: due to the specific oxidative microenvironment of tumor, Pt(IV) was intelligently activated by endogenous responsive-blue luminescence of Lu. This strategy completely avoided the limitation of poor responsiveness of prodrug with external light. Both *in vitro* and *in vivo* experimnets showed that Pt(IV) remained inert in the reducing environment, ensuring its good biological safety, and achieved the responsive and efficient killing effects on target sites. All of these results suggested that photoactivation of Pt(IV) prodrugs using endogenous light is a new pathway for the design of platinum prodrug. Meanwhile, the luminescence-activated strategy can provide specific light wave or energy at the target site, and can be used for the design of various photosensitive materials, such as photo-crosslinkable hydrogel and photodynamic therapy, to achieve intelligent *in situ* activation with broad application prospects.

Declaration of competing interest

The authors declare that they have no known competing financial interests or personal relationships that could have appeared to influence the work reported in this paper.

Acknowledgments

This study was supported by the National Natural Science Foundation of China (Nos. 32201171 and 82372115) and the Science and Technology Program of Guangzhou (No. 202102021266).

Supplementary materials

Supplementary material associated with this article can be found, in the online version, at doi:10.1016/j.cclet.2023.109134.

References

[1] S. Ghosh, Bioorg. Chem. 88 (2019) 102925.
[2] C. Zhang, C. Xu, X. Gao, et al., Theranostics 12 (2022) 2115–2132.
[3] T.C. Johnstone, K. Suntharalingam, S.J. Lippard, Chem. Rev. 116 (2016) 3436–3486.
[4] S. Zhang, X. Wang, Z. Guo, Rational design of anticancer platinum(IV) prodrugs, in: P.J. Sadler, R. van Eldik (Eds.), Advances in Inorganic Chemistry, Academic Press, Pittsburgh, 2020, pp. 149–182.
[5] N.J. Farrer, J.A. Woods, L. Salassa, et al., Angew. Chem. Int. Ed. 49 (2010) 8905–8908.
[6] Q. Chen, Y. Yang, X. Lin, et al., Chem. Commun. 54 (2018) 5369–5372.
[7] S. He, C. Li, Q. Zhang, et al., ACS Nano 12 (2018) 7272–7281.
[8] R. Weissleder, Nat. Biotechnol. 19 (2001) 316–317.
[9] Z. Wang, N. Wang, S.C. Cheng, et al., Chem 5 (2019) 3151–3165.
[10] Z. Deng, N. Wang, Y. Liu, et al., J. Am. Chem. Soc. 142 (2020) 7803–7812.
[11] D. Zhou, J. Guo, G.B. Kim, et al., Adv. Healthc. Mater. 5 (2016) 2493–2499.
[12] Y. Min, J. Li, F. Liu, et al., Angew. Chem. Int. Ed. 53 (2014) 1012–1016.
[13] Y. Dai, H. Xiao, J. Liu, et al., J. Am. Chem. Soc. 135 (2013) 18920–18929.

[14] D. Jia, X. Ma, Y. Lu, et al., Chin. Chem. Lett. 32 (2021) 162–167.
[15] C. Hu, Y. Song, Y. Zhang, et al., Acta Pharm. Sin. B 13 (2023) 2176–2187.
[16] S. Luo, C. Liang, Q. Zhang, et al., Chin. Chem. Lett. 34 (2023) 107666.
[17] T. Li, Y. Zhang, J. Zhu, et al., Adv. Mater. 35 (2023) e2210201.
[18] H.S. Alshetaiwi, S. Balivada, T.B. Shrestha, et al., J. Photochem. Photobiol. B 127 (2013) 223–228.
[19] H. Zheng, C. Yuan, J. Cai, et al., J. Nanobiotechnol. 20 (2022) 134.
[20] N. Zhang, K.P. Francis, A. Prakash, et al., Nat. Med. 19 (2013) 500–505.
[21] X. Xu, H. An, D. Zhang, et al., Sci. Adv. 5 (2019) eaat2953.
[22] H. An, C. Guo, D. Li, et al., ACS Appl. Mater. Interfaces 12 (2020) 17230–17243.
[23] T.P. Szatrowski, C.F. Nathan, Cancer Res. 51 (1991) 794–798.